International Journal of Bifurcation and Chaos, Vol. 28, No. 7 (2018) 1850082 (12 pages)

DOI: 10.1142/S0218127418500827

Vibrational Resonance in an Overdamped System with a Fractional Order Potential Nonlinearity

Jianhua Yang
School of Mechatronic Engineering,
China University of Mining and Technology,
Xuzhou, Jiangsu 221116, P. R. China
Department of Mechanical Engineering, University of Michigan,
Ann Arbor, MI 48109, USA
Jiangsu Key Laboratory of Mine Mechanical and Electrical Equipment,
China University of Mining and Technology,
Xuzhou 221116, P. R. China

Dawen Huang*
School of Mechatronic Engineering,
China University of Mining and Technology,
Xuzhou, Jiangsu 221116, P. R. China
dawenhuang@cumt.edu.cn

Miguel A. F. Sanjuán
Departamento de Física, Universidad Rey Juan Carlos,
Tulipán s/n, 28933 Móstoles, Madrid, Spain
Department of Applied Informatics, Kaunas University of Technology,
Studentu 50-415, Kaunas LT-51368, Lithuania
Institute for Physical Science and Technology, University of Maryland,
College Park, Maryland 20742, USA

Houguang Liu
School of Mechatronic Engineering,
China University of Mining and Technology,
Xuzhou, Jiangsu 221116, P. R. China

Received November 13, 2017; Revised April 22, 2018

We investigate the vibrational resonance by the numerical simulation and theoretical analysis in an overdamped system with fractional order potential nonlinearities. The nonlinearity is a fractional power function with deflection, in which the response amplitude presents vibrational resonance phenomenon for any value of the fractional exponent. The response amplitude of vibrational resonance at low-frequency is deduced by the method of direct separation of slow and fast motions. The results derived from the theoretical analysis are in good agreement with those of numerical simulation. The response amplitude decreases with the increase of the fractional exponent for weak excitations. The amplitude of the high-frequency excitation can induce the vibrational resonance to achieve the optimal response amplitude. For the overdamped systems, the nonlinearity is the crucial and necessary condition to induce vibrational resonance. The response amplitude in the nonlinear system is usually not larger than that in the corresponding

*Author for correspondence

linear system. Hence, the nonlinearity is not a sufficient factor to amplify the response to the low-frequency excitation. Furthermore, the resonance may be also induced by only a single excitation acting on the nonlinear system. The theoretical analysis further proves the correctness of the numerical simulation. The results might be valuable in weak signal processing.

Keywords: Vibrational resonance; fractional order nonlinearity; biharmonic excitations.

1. Introduction

Vibrational resonance (VR) is a typical nonlinear phenomenon of the nonlinear systems subjected to a low-frequency and a high-frequency excitation. When VR occurs, the response of a system to the low-frequency excitation can be amplified by the high-frequency excitation [Landa & McClintock, 2000]. Nonlinear systems subjected to biharmonic excitations are widely used in science and engineering fields. Hence, VR has been investigated in a variety of disciplines since it was proposed [Rajasekar & Sanjuán, 2016; Yang, 2016].

To our knowledge, on all works of VR, the nonlinearity of the considered system is usually a power function with an integer exponent. One reason for choosing a nonlinearity with an integer exponent is due to the simplicity in the modeling. In view of mathematical problems, the nonlinearity may be presented in a power function with a fractional exponent. There are many references discussing this issue [Kwuimy & Nbendjo, 2011; Li *et al.*, 2012; Zhang *et al.*, 2016]. In order to understand the VR phenomenon further, we will study the VR phenomenon in nonlinear systems with a fractional order potential nonlinearity. To make the problem simpler, we consider the typical overdamped system with a fractional order potential nonlinearity, which is as follows.

$$\frac{dx(t)}{dt} - ax(t) + bx(t)|x(t)|^{\alpha-1} = f\cos(\omega t) + F\cos(\Omega t). \tag{1}$$

In Eq. (1), $f\cos(\omega t)$ and $F\cos(\Omega t)$ represent low-frequency and high-frequency excitations respectively, i.e. $\omega \ll 1$, $\Omega \gg \omega$. The system parameters a and b have the same order of magnitude of 1, and $a > 0$, $b > 0$. The nonlinearity exponent α can be an integer or a fractional number and $\alpha > 1$. As to the nonlinearity in Eq. (1), it is usually used to model the nonlinear part of a stress-strain relationship of many materials [Cveticanin, 2009; Kwuimy *et al.*, 2015]. The VR in the traditional bistable system can be considered as the special case of Eq. (1). Since the VR theory has potential values in engineering fields, such as in energy harvesting [Coccolo *et al.*, 2014], signal processing [Liu *et al.*, 2017b; Jia *et al.*, 2018], mechanical fault diagnosis [Liu *et al.*, 2017a], etc., it is important to find a nonlinear model with higher VR efficiency than that in the traditional bistable system. In other words, an appropriate value of the fractional exponent should be sought to realize a better nonlinear system. This is the focus of this paper. Moreover, we consider the nonlinear model with more physical meanings as a signal processor. We aim to amplify the weak low-frequency signal by VR method in an optimal nonlinear system to a great extent.

For some special nonlinear systems, the VR phenomenon is usually studied analytically by the method of direct separation of slow and fast motions [Blekhman, 2000; Thomsen, 2003]. Therefore, for the nonlinear model shown in Eq. (1), we also adopt the method of direct separation of slow and fast motions to analyze the VR phenomenon. Thus, we study here the VR by the numerical simulation and theoretical analysis. The outline of the paper is organized as following. In Sec. 2, we will discuss the VR phenomenon by the numerical simulation. In Sec. 3, we will study the VR phenomenon by the theoretical analysis. The effects of the high-frequency excitation and the nonlinearity on the VR response will be discussed in detail in Secs. 2 and 3. In the last section, the main results of this work are described. In addition, a simple comparison is made in the VR and stochastic resonance based on the same overdamped system with a fractional order potential nonlinearity.

2. The VR Phenomenon by Numerical Simulation

In this section, we will investigate in detail the VR phenomenon in the fractional power system subjected to a single harmonic excitation and two harmonic excitations, respectively.

2.1. *The response of the system subjected to a single harmonic excitation*

The potential of Eq. (1) is a fractional power function with deflection

$$V(x) = -\frac{a}{2}x^2 + \frac{b}{\alpha+1}|x|^{\alpha+1}. \tag{2}$$

It is a bistable system when $\alpha > 1$ no matter if α is an integer or a noninteger number. The form of the potential is independent of the exponent of the nonlinearity. It is very similar to the traditional bistable potential. There are three equilibria for the potential in Eq. (2). Specifically, one unstable equilibrium $x_0 = 0$ and two stable equilibria $x_{1,2} = \pm(\frac{a}{b})^{\frac{1}{\alpha-1}}$. When $a = 1$ and $b = 1$, the plots of the potential function are given in Fig. 1 for different values of the fractional exponent.

To analyze the VR phenomenon, we need to study the response amplitude at the low-frequency, which is defined by

$$Q(\omega) = \frac{\sqrt{Q_{\sin}^2(\omega) + Q_{\cos}^2(\omega)}}{f}, \tag{3}$$

where

$$Q_{\sin}(\omega) = \frac{2}{rT}\int_0^{rT} x(t)\sin(\omega t)dt,$$

$$Q_{\cos}(\omega) = \frac{2}{rT}\int_0^{rT} x(t)\cos(\omega t)dt.$$

The value r is a positive integer number which should be large enough, while T is the period of the low-frequency excitation. If only one excitation is considered, the definition of the response amplitude at the excitation frequency is similar to that in Eq. (3).

In Figs. 2 and 3, the response amplitude under a single harmonic excitation is plotted respectively. In Figs. 2(a) and 2(b), Eq. (1) is only subjected to the low-frequency excitation. In Figs. 3(a) and 3(b), Eq. (1) is only subjected to the high-frequency excitation. In all subplots of Figs. 2 and 3, there is no divergence with the variation of the nonlinearity exponent. Another fact can be found in Figs. 2 and 3. Specifically, the resonance can be induced by

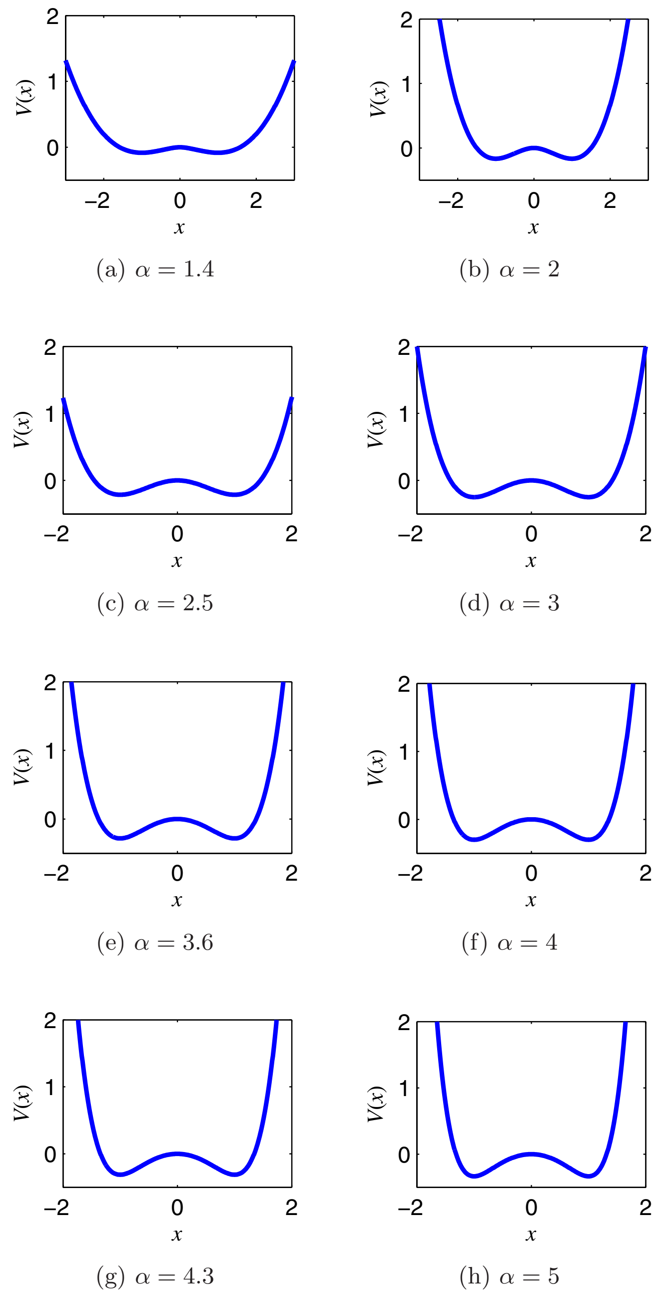

(a) $\alpha = 1.4$ (b) $\alpha = 2$ (c) $\alpha = 2.5$ (d) $\alpha = 3$ (e) $\alpha = 3.6$ (f) $\alpha = 4$ (g) $\alpha = 4.3$ (h) $\alpha = 5$

Fig. 1. The potential of Eq. (1) under different values of the exponent α, $a = 1$ and $b = 1$.

the harmonic excitation amplitude. It is an important result in the nonlinear system. As is known to all, in the linear system, the response amplitude is independent of the excitation amplitude.

2.2. *The response of the system subjected to two harmonic excitations*

In Fig. 4, under different values of f and α, the plots of the response amplitude versus the control

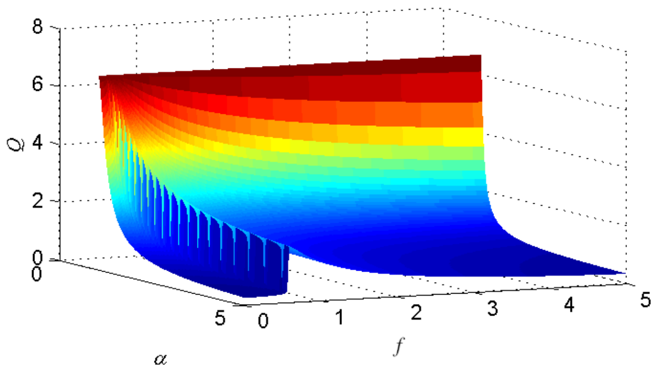

(a)

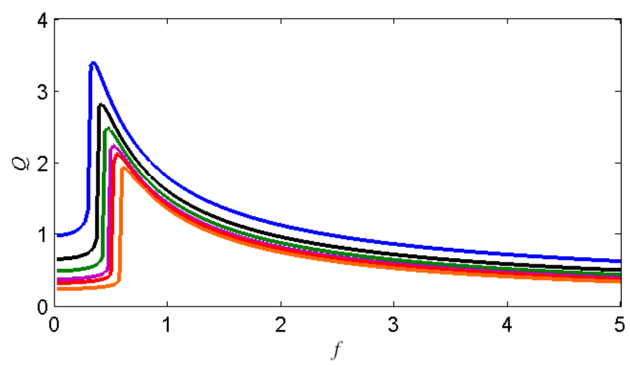

(b)

Fig. 2. The response amplitude of Eq. (1) subjected to a single low-frequency harmonic excitation, $a = 1$, $b = 1$, $\omega = 0.15$, $F = 0$. The curves in (a) and (b): $\alpha = 2$, $\alpha = 2.5$, $\alpha = 3$, $\alpha = 3.6$, $\alpha = 4$, $\alpha = 5$.

parameter F are given. In Fig. 4(a), when $\alpha = 1.4$ and $f = 0.3$, the VR phenomenon is not explicit. On all other curves in Fig. 4, the VR phenomenon is more evident. More importantly, the response of the system will not be divergent no matter if the exponent of the nonlinearity is an integer or a non-integer number. The reason lies in the fact that the equivalent potential of Eq. (1) will always have at least one stable equilibrium. Therefore, the excitation cannot induce the response to be divergent in Fig. 4.

In Fig. 5, the exponent of the nonlinearity is considered as a control variable and the curves of Q–α are plotted under different values of the strength of the low-frequency excitation. Two important facts are shown there. On the one hand, the response amplitude Q decreases with the increase of the exponent value α. On the other hand, the response will not be divergent for any value of α. In other words, the response of Eq. (1) is not easy to be divergent.

In Fig. 6, we plot the curves of the response amplitude Q versus the amplitude of the high-frequency excitation for some small values of α. When $\alpha = 1$, Eq. (1) turns into a linear equation

$$\frac{dx(t)}{dt} + (b - a)x(t) = f\cos(\omega t) + F\cos(\Omega t). \tag{4}$$

The steady solution of this equation is

$$x(t) = \frac{f}{\sqrt{\omega^2 + (a-b)^2}}\cos\left(\omega t + \arctan\frac{\omega}{a-b}\right) + \frac{F}{\sqrt{\Omega^2 + (a-b)^2}}\cos\left(\Omega t + \arctan\frac{\Omega}{a-b}\right). \tag{5}$$

The response amplitude at the low-frequency is accurately calculated as

$$Q = \frac{1}{\sqrt{\omega^2 + (a-b)^2}}. \tag{6}$$

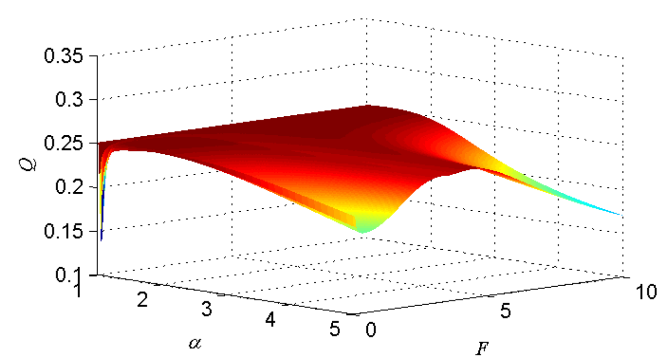

(a)

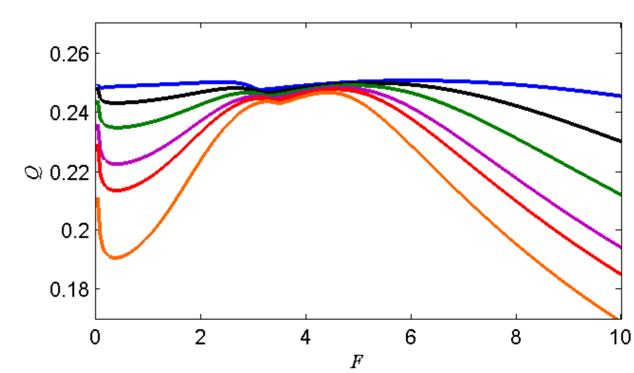

(b)

Fig. 3. The response amplitude of Eq. (1) subjected to a single high-frequency harmonic excitation, $a = 1$, $b = 1$, $f = 0$, $\Omega = 4$. The curves in (a) and (b): $\alpha = 2$, $\alpha = 2.5$, $\alpha = 3$, $\alpha = 3.6$, $\alpha = 4$, $\alpha = 5$.

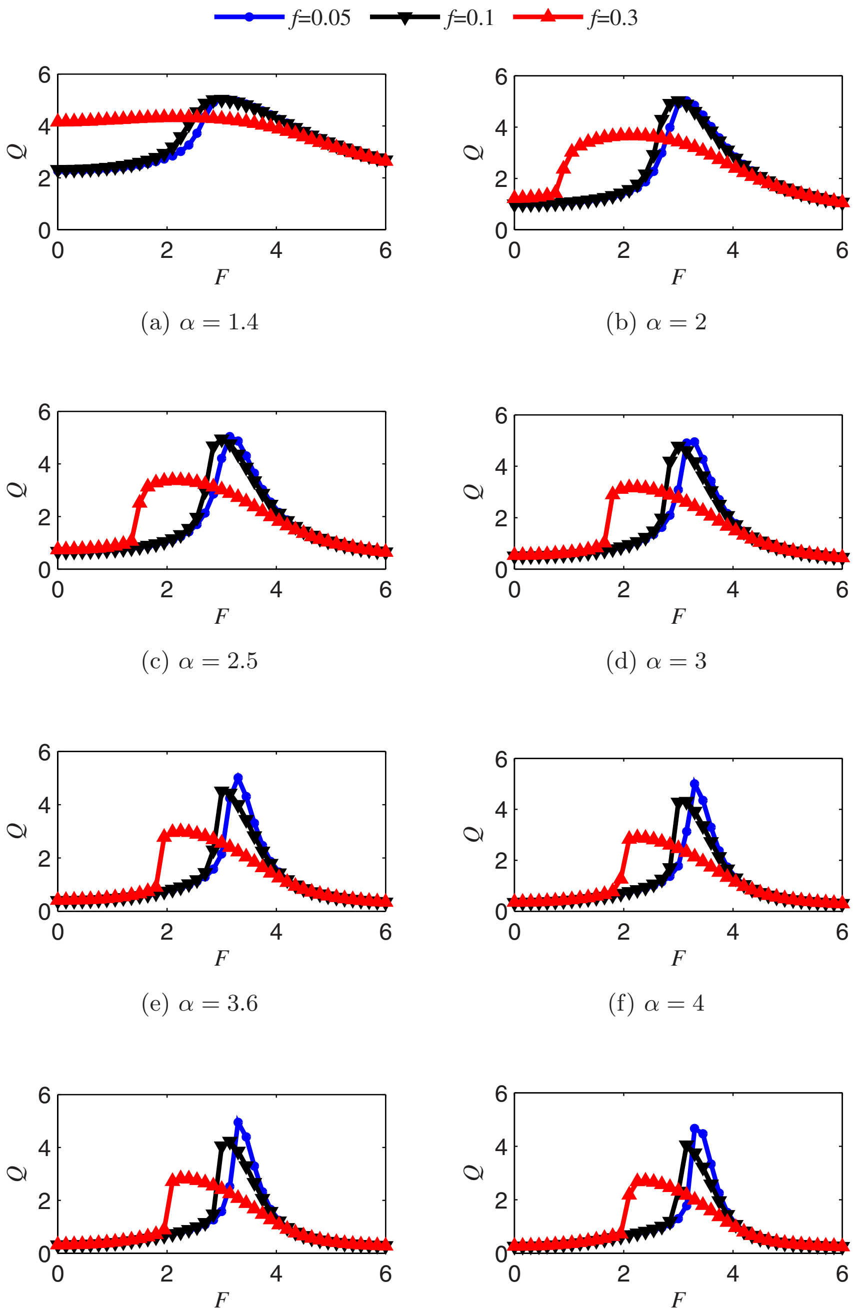

Fig. 4. The response amplitude of Eq. (1) versus the variable F when the system is subjected to two harmonic excitations. The simulation parameters are $a = 1$, $b = 1$, $\omega = 0.2$ and $\Omega = 4$.

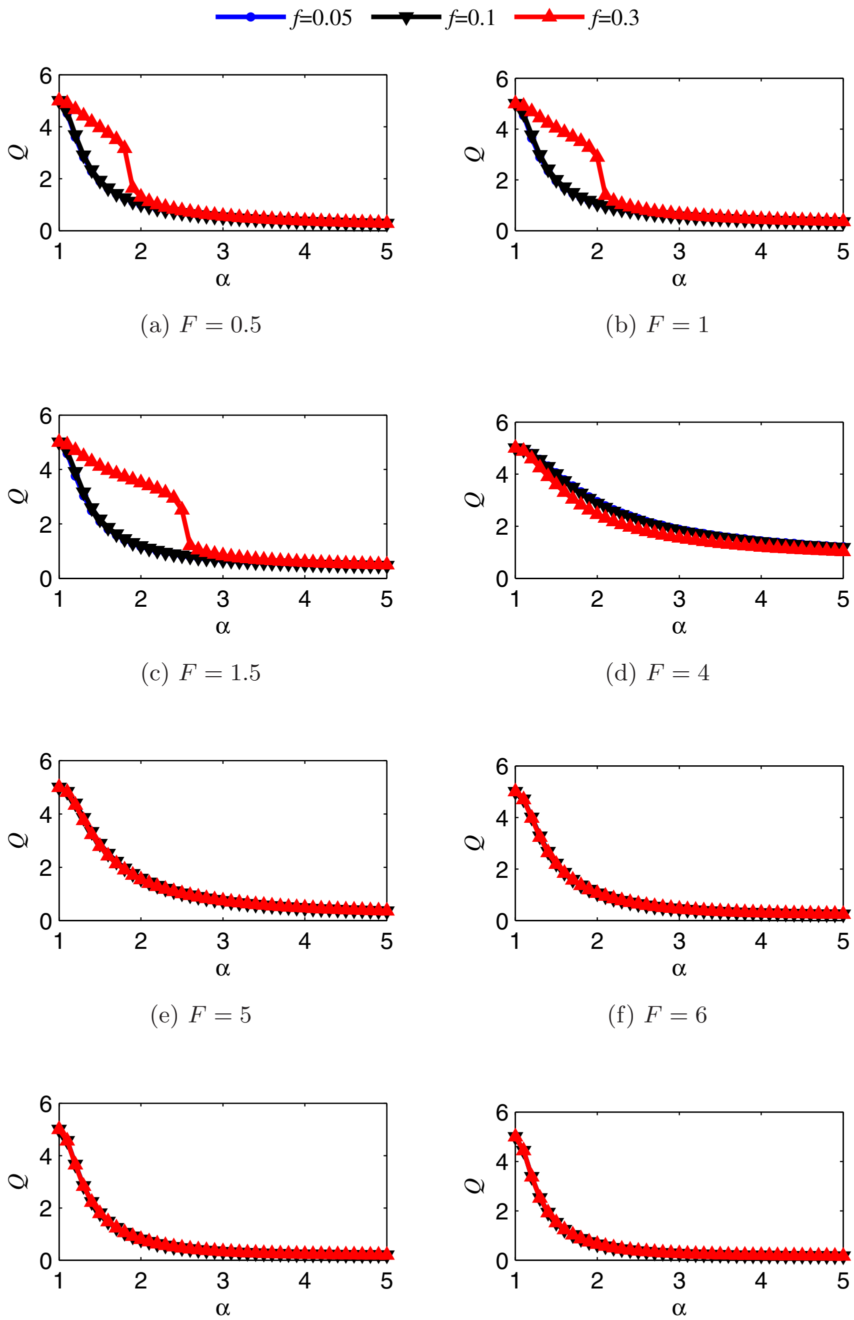

(a) $F = 0.5$ (b) $F = 1$

(c) $F = 1.5$ (d) $F = 4$

(e) $F = 5$ (f) $F = 6$

(g) $F = 7$ (h) $F = 8$

Fig. 5. The response amplitude of Eq. (1) versus the exponent α when the system is subjected to two harmonic excitations. The simulation parameters are $a = 1$, $b = 1$, $\omega = 0.2$ and $\Omega = 4$.

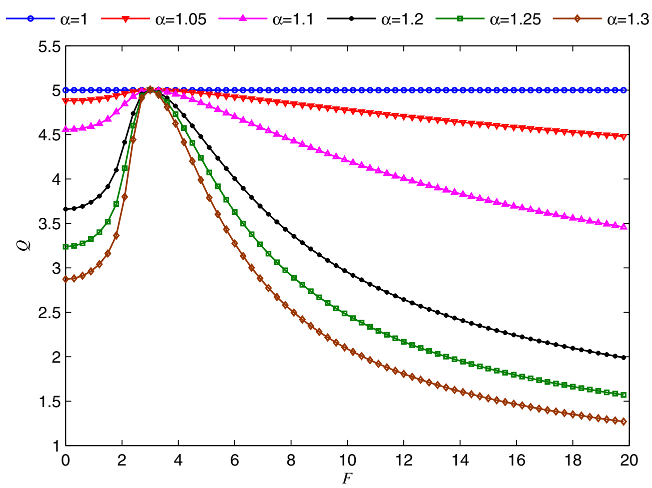

Fig. 6. The response amplitude of Eq. (1) versus the variable F when the system is subjected to two harmonic excitations. The simulation parameters are $a = 1$, $b = 1$, $f = 0.1$, $\omega = 0.2$ and $\Omega = 4$.

It is independent of the high-frequency excitation, as shown in Fig. 6. Importantly, nonlinearity is the key and the necessary condition to induce the VR phenomenon. Different from Fig. 2, the values of the resonance peaks are almost identical. These peak values approach the response amplitude of the corresponding linear system. In other words, Eq. (1) can create the response to achieve the strongest resonance.

3. The VR Phenomenon by Theoretical Analysis

In this section, in order to obtain the analytical results of Eq. (1) under two harmonic excitations, we will introduce the method of direct separation of slow and fast motions to investigate VR phenomenon.

Introducing the substitution variable

$$x(t) = X(t) + \Psi(t), \tag{7}$$

where X and Ψ are the slow and fast motions, respectively. Substituting Eq. (7) into Eq. (1), then Eq. (1) is rewritten as

$$\frac{dX}{dt} + \frac{d\Psi}{dt} = aX + a\Psi - b(X+\Psi)|X+\Psi|^{\alpha-1} + f\cos(\omega t) + F\cos(\Omega t). \tag{8}$$

Due to the presence of absolute symbol in Eq. (8), we discuss two situations.

(I) When $X(t) + \Psi(t) > 0$, Eq. (8) is expressed as

$$\frac{dX}{dt} + \frac{d\Psi}{dt} = a(X+\Psi) - b(X+\Psi)^{\alpha} + f\cos(\omega t) + F\cos(\Omega t). \tag{9}$$

According to the binomial theorem, Eq. (9) is rewritten as

$$\frac{dX}{dt} + \frac{d\Psi}{dt} = a(X+\Psi) - b\sum_{k=0}^{[\alpha]} C_{\alpha}^{k} X^{\alpha-k}\Psi^{k} + f\cos(\omega t) + F\cos(\Omega t), \tag{10}$$

where $[\bullet]$ denotes integral function towards zero. C_{α}^{k} is the binomial coefficient. The linear equation of the fast motion Ψ originates from Eq. (10) as

$$\frac{d\Psi}{dt} = a\Psi + F\cos(\Omega t). \tag{11}$$

Assuming the approximate solution of the linear differential equation (11) is $\Psi = \mu\cos(\Omega t - \theta)$, and substituting it into Eq. (11), we can attain the following results,

$$-\mu\Omega = -F\sin\theta, \quad a\mu = -F\cos\theta. \tag{12}$$

The approximate solution Ψ is calculated by squaring and summing the left- and right-hand sides of Eq. (12) respectively, which is

$$\Psi = \frac{F}{\sqrt{a^2+\Omega^2}}\cos\left(\Omega t + \arctan\frac{\Omega}{a}\right). \tag{13}$$

The approximate solution Ψ is substituted into Eq. (9), then integral operation is implemented in the interval $[0, \frac{2\pi}{\Omega}]$. In the process of integration, the variables X and f are regarded as constants.

$$\frac{dX}{dt} = aX - \frac{b\Omega}{2\pi}\sum_{k=0}^{[\alpha]}\left(C_{\alpha}^{k}X^{\alpha-k}\int_0^{\frac{2\pi}{\Omega}}\Psi^k dt\right) + f\cos(\omega t). \tag{14}$$

As we know, integral term $\int_0^{\frac{2\pi}{\Omega}}\Psi^k dt = \frac{C_k^{\frac{k}{2}}}{2^k}\mu^k\frac{2\pi}{\Omega}$ when k is 0 or an even number, and integral term $\int_0^{\frac{2\pi}{\Omega}}\Psi^k dt = 0$ when k is odd number. Hence, Eq. (14) is re-expressed as

$$\frac{dX}{dt} = aX - b\sum_{k=0}^{[\frac{\alpha}{2}]}\left(C_{\alpha}^{2k}X^{\alpha-2k}\frac{C_{2k}^{k}}{2^{2k}}\mu^{2k}\right) + f\cos(\omega t). \tag{15}$$

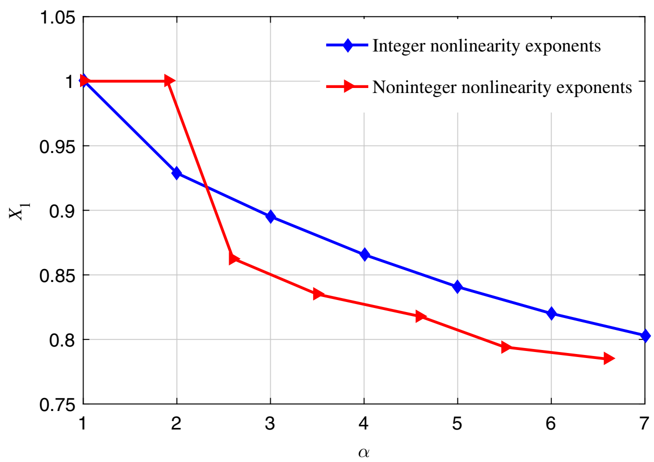

Fig. 7. The positive equilibrium points X_1 versus the nonlinearity exponents α when α is an integer or a noninteger number. The related parameters are $a = 1$, $b = 1$, $F = 1.5$, $\omega = 0.2$ and $\Omega = 4$.

We can obtain the equilibrium points for different nonlinearity exponents α by solving equation $aX - b\sum_{k=0}^{[\frac{\alpha}{2}]}(C_\alpha^{2k}X^{\alpha-2k}\frac{C_{2k}^k}{2^{2k}}\mu^{2k}) = 0$ from Eq. (15). The curves of the positive equilibrium points X_1 versus the nonlinearity exponents α are given in Fig. 7. No matter if α is the integer nonlinearity exponent or the noninteger, the value of the positive equilibrium point decreases with the increase of the nonlinearity exponent value. The system with a fractional order potential nonlinearity possesses different positive stable equilibria for different nonlinearity exponents, which indicates that the VR phenomenon is generated in a suitable bistable system by choosing an appropriate exponent value for the arbitrary low-frequency excitations. There are two stable equilibria $X_{1,2} = \pm(\frac{a}{b})^{\frac{1}{\alpha-1}}$ at $k = 0$ and $1 < \alpha < 2$, which are consistent with the results obtained directly from Eq. (2). Thus, when $a = 1$, $b = 1$ and $1 < \alpha < 2$, the positive stable equilibrium point $X_1 = 1$, is as shown in Fig. 7. Without regard to external excitation $f\cos(\omega t)$ in Eq. (15), the Taylor expansion is carried out at the positive stable equilibrium point X_1. Equation (15) is converted to

$$\frac{dX}{dt} = a(X - X_1) - b\sum_{k=0}^{[\frac{\alpha}{2}]} \times \left(C_\alpha^{2k}(\alpha - 2k)X_1^{\alpha-2k-1}\frac{C_{2k}^k}{2^{2k}}\mu^{2k}(X - X_1)\right). \tag{16}$$

Letting $y = X - X_1$, then Eq. (16) is changed to

$$\frac{dy}{dt} = \left[a - b\sum_{k=0}^{[\frac{\alpha}{2}]}\left(C_\alpha^{2k}(\alpha - 2k)X_1^{\alpha-2k-1}\frac{C_{2k}^k}{2^{2k}}\mu^{2k}\right)\right]y. \tag{17}$$

(II) When $X(t) + \Psi(t) < 0$, Eq. (8) is expressed as

$$\frac{dX}{dt} + \frac{d\Psi}{dt} = a(X + \Psi) + (-1)^\alpha b(X + \Psi)^\alpha + f\cos(\omega t) + F\cos(\Omega t). \tag{18}$$

We can attain the following Eq. (19) by using the same method shown in Eqs. (10)–(15) to deal with Eq. (18).

$$\frac{dX}{dt} = aX + (-1)^\alpha b\sum_{k=0}^{[\frac{\alpha}{2}]}\left(C_\alpha^{2k}X^{\alpha-2k}\frac{C_{2k}^k}{2^{2k}}\mu^{2k}\right) + f\cos(\omega t). \tag{19}$$

Without consideration of the external excitation $f\cos(\omega t)$ in Eq. (19), the Taylor expansion is implemented at the negative stable equilibrium point X_2. Equation (19) is converted to

$$\frac{dX}{dt} = a(X + X_2) + (-1)^\alpha b\sum_{k=0}^{[\frac{\alpha}{2}]} \times \left(C_\alpha^{2k}(\alpha - 2k)X_2^{\alpha-2k-1}\frac{C_{2k}^k}{2^{2k}}\mu^{2k}(X + X_2)\right). \tag{20}$$

We know that two stable equilibria of the bistable system are symmetric, therefore, $X_2 = -X_1$. Substituting $y = X + X_2$ into Eq. (20), which is then converted to

$$\frac{dy}{dt} = \left[a - b\sum_{k=0}^{[\frac{\alpha}{2}]}\left(C_\alpha^{2k}(\alpha - 2k)X_1^{\alpha-2k-1}\frac{C_{2k}^k}{2^{2k}}\mu^{2k}\right)\right]y. \tag{21}$$

It is easy to find that Eq. (17) is exactly the same as Eq. (21). In other words, the results of direct separation of slow and fast motions are identical in the case of both $X(t) + \Psi(t) > 0$ and $X(t) + \Psi(t) < 0$.

Letting

$$C_r = a - b\sum_{k=0}^{[\frac{\alpha}{2}]}\left(C_\alpha^{2k}(\alpha - 2k)X_1^{\alpha-2k-1}\frac{C_{2k}^k}{2^{2k}}\mu^{2k}\right),$$

then Eqs. (17) and (21) are both converted to a linear first order differential equation under a harmonic excitation.

$$\frac{dy}{dt} = C_r y + f\cos(\omega t). \tag{22}$$

We can obtain the solution of the linear differential equation (22), which is

$$y = \frac{f}{\sqrt{\omega^2 + C_r^2}} \cos\left(\omega t + \arctan\frac{\omega}{C_r}\right). \tag{23}$$

The solution y of the linear differential equation is also the resonance response of the nonlinear system with a fractional order potential nonlinearity as shown in Eq. (1). The response amplitude at the low-frequency is accurately calculated as

$$Q = \frac{1}{\sqrt{\omega^2 + C_r^2}}. \tag{24}$$

In the process of theoretical analysis, the term $(X + \Psi)^\alpha$ is expanded according to the binomial theorem. In the expression of C_r, $[\frac{\alpha}{2}] = 0$ when $1 < \alpha < 2$, hence, C_r is independent of the high-frequency excitation amplitude F. It is in accordance with the resonance response of a linear system. At $\alpha = 2$ and $k = 1$, the term $\alpha - 2k = 0$, C_r is still independent of the excitation amplitude F. The binomial theorem used in the theoretical analysis has some limitations for the case of smaller nonlinearity exponents. The larger the nonlinear exponent, the more accurate the value

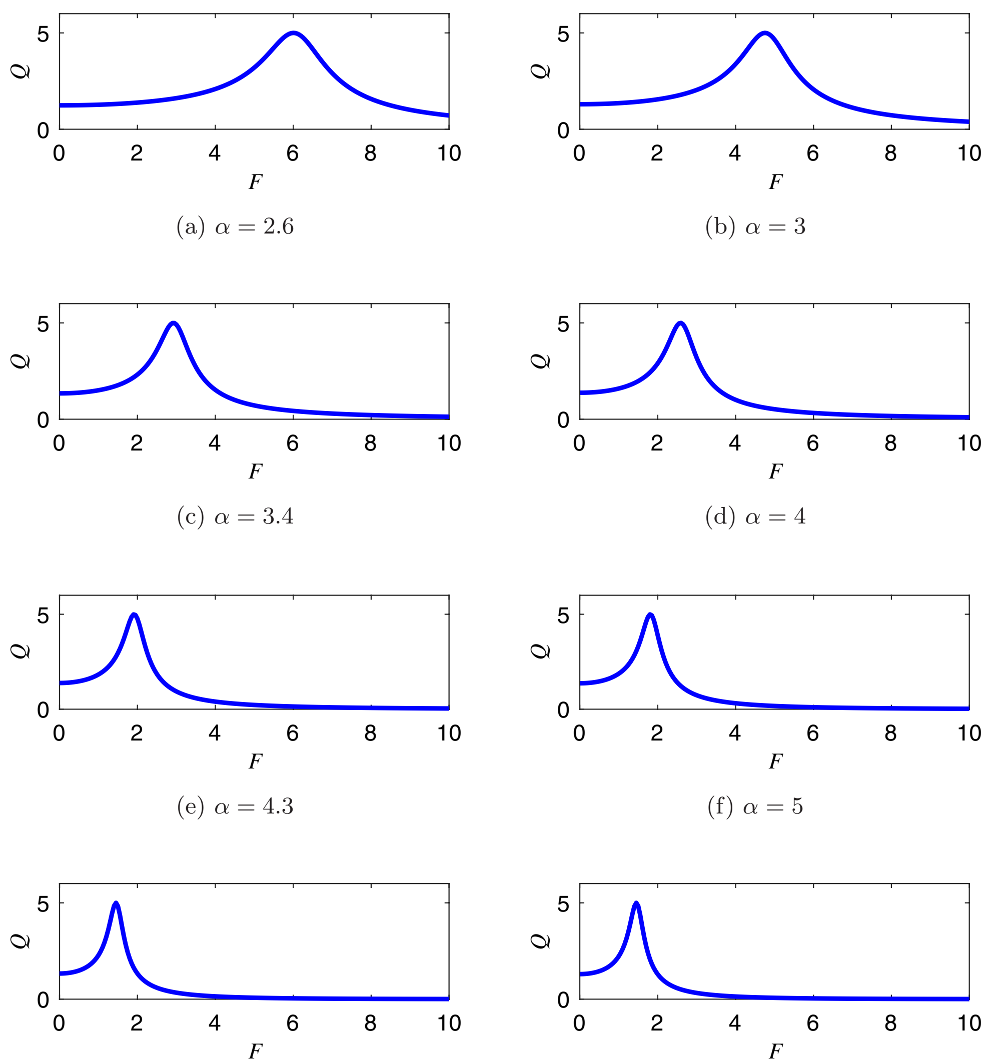

(a) $\alpha = 2.6$ (b) $\alpha = 3$ (c) $\alpha = 3.4$ (d) $\alpha = 4$ (e) $\alpha = 4.3$ (f) $\alpha = 5$ (g) $\alpha = 5.6$ (h) $\alpha = 6$

Fig. 8. The response amplitude Q obtained by the theoretical analysis versus the high-frequency excitation amplitude F. The involved parameters are $a = 1.5, b = 0.4, \Omega = 4$ and $\omega = 0.2$.

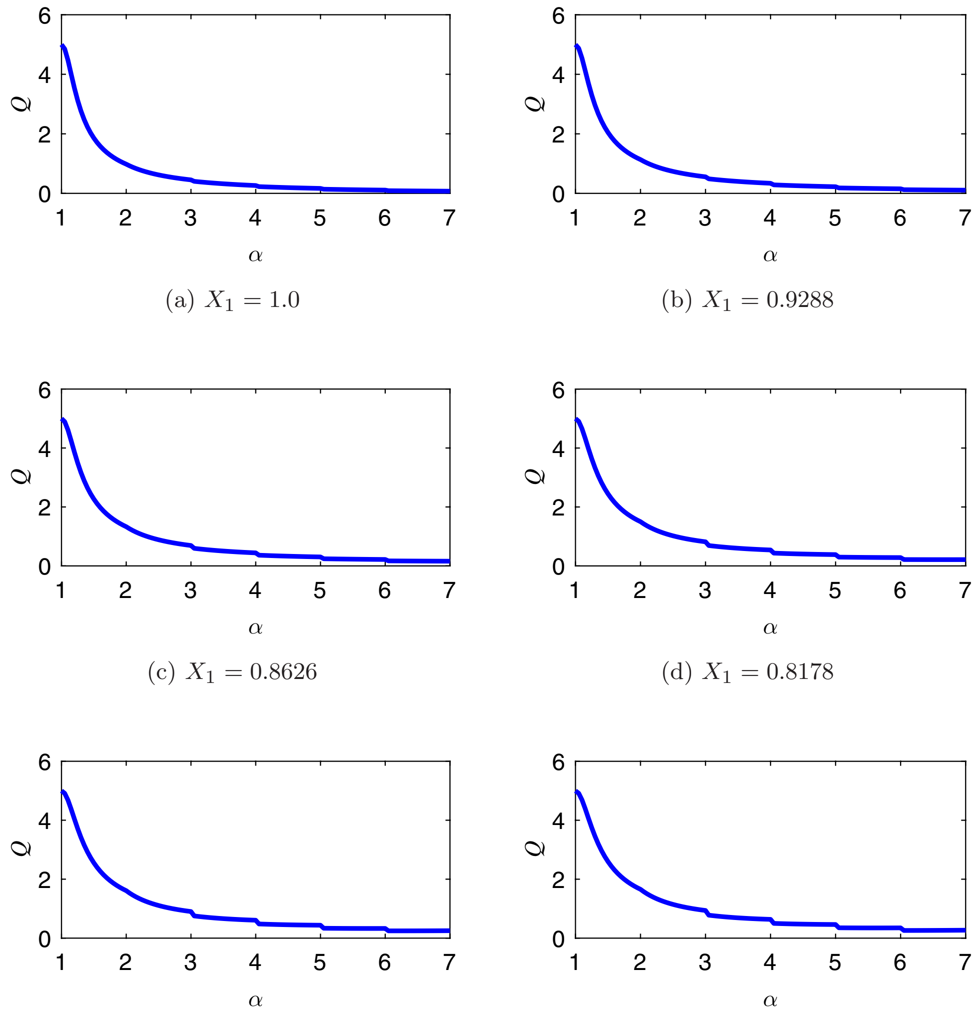

(a) $X_1 = 1.0$

(b) $X_1 = 0.9288$

(c) $X_1 = 0.8626$

(d) $X_1 = 0.8178$

(e) $X_1 = 0.7941$

(f) $X_1 = 0.7848$

Fig. 9. The response amplitude Q obtained by the theoretical analysis depends on the nonlinearity exponent α under different variable X_1. The involved parameters are $a = 1$, $b = 1$, $\Omega = 4$, $\omega = 0.2$ and $F = 1.5$.

of the response amplitude. In fact, the nonlinearity is existent for $1 < \alpha \leq 2$. For the situation of larger exponents, the plots of the response amplitude Q derived by the theoretical analysis versus the amplitude of high-frequency excitation are shown in Fig. 8 for different exponents α. For each nonlinearity exponent, there is an optimal high-frequency excitation amplitude achieving the optimal response of VR. As the nonlinearity exponent increases, the amplitude of the high-frequency excitation required to generate the optimal VR decreases. The results of the theoretical analysis are in agreement with those of the numerical simulation shown in Fig. 4.

The response amplitude Q depends on the exponent α for different positive stable equilibria X_1, as shown in Fig. 9. The values of the stable equilibria are selected from Fig. 7. The response amplitude Q decreases with an increasing exponent value α. The results are completely identical with those displayed in Fig. 5. The theoretical analysis proves the correctness of the numerical simulation.

4. Conclusions

The VR phenomenon is investigated by the numerical simulation and theoretical analysis in the overdamped system with the fractional order potential nonlinearity. The nonlinearity is a fractional power function with deflection. To our knowledge, the corresponding results on VR in the fractional power system have not been reported earlier in previous works. There are some new and interesting results.

The nonlinearity is in a fractional power function of deflection form, there are four important findings in the nonlinear system. First, the response will not be divergent no matter if the excitation is a single harmonic excitation or two-frequency harmonic excitations. Second, the VR phenomenon exists for any value of the fractional exponent. Third, the response amplitude versus the fractional exponent is a decreasing function. Fourth, the nonlinearity is the key and necessary factor to induce the VR phenomenon, however, it is not the sufficient factor to amplify the response to the weak low-frequency excitation. The peaks of the VR curve are usually smaller than the response amplitude of the corresponding linear system. The results of theoretical analysis are in good agreement with those of numerical simulation, which verifies the correctness of the conclusions.

Through the results in this paper, we find that the system which possesses a fractional power function with deflection is an excellent system that can amplify the weak low-frequency excitation to a great extent. Besides, the response of the system is not easy to be divergent. We think that our findings might be useful in the signal processing fields.

In the present work, two harmonic signals are considered as excitations of the nonlinear system. If one of the excitations is a noise, the VR is replaced by the famous stochastic resonance (SR). SR in overdamped system with fractional power nonlinearity is researched in our previous work [Yang *et al.*, 2017], the results of which are similar to those of VR. In the SR, the response of the system also closely depends on the fractional exponent and noise intensity. The spectral amplification factor decreases with the increase of fractional exponent, which is identical to VR as shown in Fig. 5. The existence of optimal noise intensity (amplitude of the high-frequency excitation) in SR (VR) optimizes the response of the system no matter if α is an integer or a noninteger number. The results obtained from the SR analysis also indicate that the nonlinearity is the key and necessary condition to induce SR, however, it is not the sufficient condition to amplify the weak low-frequency signal. Both in SR and VR analyses, the overdamped system with fractional deflection nonlinearity has a good performance.

Acknowledgments

J. H. Yang acknowledges the National Natural Science Foundation of China (Grant No. 11672325), and the Priority Academic Program Development of Jiangsu Higher Education Institutions, Top-notch Academic Programs Project of Jiangsu Higher Education Institutions. M. A. F. Sanjuán acknowledges the Spanish Ministry of Economy and Competitiveness (Grant No. FIS2016-76883-P), and the jointly sponsored financial support by the Fulbright Program and the Spanish Ministry of Education (Program No. FMECD-ST-2016).

References

Blekhman, I. I. [2000] *Vibrational Mechanics*: *Nonlinear Dynamic Effects*, *General Approach*, *Applications* (World Scientific, Singapore).

Coccolo, M., Litak, G., Seoane, J. M. & Sanjuán, M. A. F. [2014] "Energy harvesting enhancement by vibrational resonance," *Int. J. Bifurcation and Chaos* **24**, 1430019-1–7.

Cveticanin, L. [2009] "Oscillator with fraction order restoring force," *J. Sound Vibr.* **320**, 1064–1077.

Jia, P. X., Wu, C. J., Yang, J. H., Sanjuán, M. A. F. & Liu, G. X. [2018] "Improving the weak aperiodic signal by three kinds of vibrational resonance," *Nonlin. Dyn.* **91**, 2699–2713.

Kwuimy, C. K. & Nbendjo, B. N. [2011] "Active control of horseshoes chaos in a driven Rayleigh oscillator with fractional order deflection," *Phys. Lett. A* **375**, 3442–3449.

Kwuimy, C. K., Litak, G. & Nataraj, C. [2015] "Nonlinear analysis of energy harvesting systems with fractional order physical properties," *Nonlin. Dyn.* **80**, 491–501.

Landa, P. S. & McClintock, P. V. E. [2000] "Vibrational resonance," *J. Phys. A*: *Math. Gen.* **33**, L433–L438.

Li, H., Liao, X., Ullah, S. & Xiao, L. [2012] "Analytical proof on the existence of chaos in a generalized Duffing-type oscillator with fractional-order deflection," *Nonlin. Anal.*: *Real World Appl.* **13**, 2724–2733.

Liu, Y., Dai, Z., Lu, S., Liu, F., Zhao, J. & Shen, J. [2017a] "Enhanced bearing fault detection using step-varying vibrational resonance based on Duffing oscillator nonlinear system," *Shock Vibr.* **2017**, 5716296.

Liu, H. G., Liu, X. L., Yang, J. H., Sanjuán, M. A. & Cheng, G. [2017b] "Detecting the weak high-frequency character signal by vibrational resonance in the Duffing oscillator," *Nonlin. Dyn.* **89**, 2621–2628.

Rajasekar, S. & Sanjuán, M. A. F. [2016] *Nonlinear Resonances* (Springer, Switzerland).

Thomsen, J. J. [2003] *Vibrations and Stability*: *Advanced Theory*, *Analysis*, *and Tools* (Springer, Berlin, Heidelberg).

Yang, J. H. [2016] *Bifurcation and Resonance in Fractional-Order Systems* (Science Press, Beijing).

Yang, J. H., Sanjuán, M. A., Chen, P. P. & Liu, H. G. [2017] "Stochastic resonance in overdamped systems with fractional power nonlinearity," *Eur. Phys. J. Plus* **132**, 432.

Zhang, J., Hu, W. & Ma, Y. [2016] "The Klein–Gordon–Zakharov equations with the positive fractional power terms and their exact solutions," *Pramana* **87**, 93-1–9.